

PRECAST UNBONDED PRESTRESSED CONCRETE BRIDGE COLUMNS FOR SEISMIC APPLICATIONS

Ryo Yamashita¹ and David H. Sanders²

Abstract

Shake table testing and analysis were conducted to investigate the seismic performance of precast unbonded prestressed concrete columns. Shake table testing was conducted using the Kobe Earthquake motion. The specimen performed very well with essentially no residual displacement and only limited spalling at the base.

A parametric study was conducted with a nonlinear two-dimensional finite element push-over analysis. An equation to estimate the strain in the prestressing steel was proposed. Unbonded prestress columns can be designed to provide excellent drift capacity with limited permanent displacements.

Introduction

The application of precast segmental construction to concrete bridges has increased because of its efficiency and high quality. Precast segmental construction can reduce work at a construction site. Therefore, precast segmental construction makes construction periods shorter. As a result, the construction cost of the precast segmental method could be possibly lower than that of the other conventional construction methods. Also, concrete bridges with high quality need less maintenance, and consequently, the life cycle cost of precast segmental bridges will be lower than that of conventional concrete bridges. The fast construction with precast elements is especially useful for construction in an urban setting where long traffic control cannot be permitted. The main objective of this research was to investigate the seismic performance of precast unbonded prestressed concrete columns with the expectation of small residual displacements and easy repair after a large earthquake.

The current specifications (AASHTO 1999 and AASHTO 2002) provide limited guidance for precast column system, especially in high seismic zones. Limited research regarding seismic performance of the unbonded prestressed concrete columns is available. To apply unbonded prestressed precast column system in high seismic zones, a practical design method must be developed. Estimating the strain change in the prestressing steel is difficult because strain compatibility is no longer valid. It is essential to understand how the structure behaves under seismic loads for actual design.

¹ Senior Engineer, Engineering Dept., PC Bridge Co., Ltd., Tokyo, Japan

² Associate Professor, Dept. of Civil Engineering, University of Nevada, Reno

Specimen Design and Construction

The design of the specimen was based on a full-scale prototype. The cross section of the column in the AASHTO-PCI-ASBI Standards (AASHTO-PCI-ASBI 2002) was used for the basic dimensions of the prototype structure cross section, and the compressive strength of concrete was 35 MPa (5 ksi). The scaling factor of the specimen was one-fourth, which was necessary to match the capacity of the specimen with that of the test equipment. Front and side views of the specimen are shown in **Fig. 1** and the column cross section with the reinforcement is shown in **Fig. 2**. No conventional reinforcement crosses the joints of the column. An aspect ratio of four was taken in the weak/testing direction to investigate the flexural characteristics of the column. The detailed description about the specimen design is provided in a research report by the authors (Yamashita and Sanders 2005).

The specimen was constructed by match casting, where the previous constructed segment was used as the form of the next segment. The prestressing steel was set to the anchorage system prior to concrete casting of the footing using a fixed-end anchorage system. After the construction of the segments, the footing, the segments and the head were put together using epoxy adhesive for segmental bridges. Immediately after assembling the specimen, the prestressing force was applied. The pump pressure and the values of the prestressing strain gauges were checked against the calibrations done prior to assembly. The target strain determined by the design was 5600 $\mu\epsilon$ that corresponded to 1100 MPa (160 ksi).

Test Setup and Procedure

The test setup is shown in **Fig. 3**. This test system was developed at the University of Nevada, Reno to simulate structures under earthquake motions (Laplace et al 2005). The weight of the superstructure is applied by center-hole jacks and the inertial force is applied through a rigid link that connects to the mass rig. The mass rig holds 356 kN (80 kips) of concrete and has 89 kN (20 kips) of effective rotational mass. The mass rig is a pinned structure that gets its stability from the specimen. As the shake table and specimen move together, the mass rig creates the inertial force.

The shake table testing was conducted with the Kobe Earthquake motion recorded at the Kobe Oceanic Meteorological Observatory. The shake table testing consisted of fifteen runs, where the amplitude of acceleration from the Kobe motion was increased until failure. The maximum table accelerations were from 0.05g to 1.27g while the original peak ground acceleration of the Kobe motion was 0.82g. The length of the record was scaled by the square root of the scale factor of the specimen.

Observed Behavior

Table 1 shows the observed behavior at selected runs. During Run 5, joint opening at the bottom of the column was observed. The first crushing of the cover concrete was confirmed after Run 11 on the south side of the first segment. The spalling of the cover concrete was observed after Run 13. During Run 14, the cover

concrete at the south side completely spalled from the bottom of the column and the transverse reinforcement was exposed as shown in **Fig. 4**. Also, the anchorage plate of the prestressing steel at the center of the north side, strand No.1, popped out during Run 14. The strand numbers are shown in **Fig. 2**. Since this behavior occurred when the strand was in tension, it could be assumed that slippage at the wedges in the anchorage plate occurred during Run 14 and the anchorage plate popped out due to the impact of the slippage.

Two more anchorage plates on the north side, which were strands No. 9 and No. 11, popped out during Run 15 for the same reason as strand No. 1. **Fig. 5** shows the anchorage plates after testing. After Run 15, damage of the core concrete was also observed at the corners of the section although no significant damage was found. No significant residual displacement was observed throughout all runs, as expected. The test was stopped after Run 15 because the specimen became unstable due to popping out of the anchorages.

Force and Displacement Histories

The accumulated force-displacement hysteresis curve for all runs is shown in **Fig. 6**. The lateral displacement was calculated by subtracting the absolute table displacement from the absolute column displacement. The negative sign indicates movement in the south direction. The force was the recorded data by the load cell placed in the link to the mass rig. Abrupt reduction of the force occurred in the south/negative direction at -61 mm (-2.4 in) during Run 14 due to the slippage at the wedges of strand No. 1, as described in the previous section. Additional force reduction happened due to the slippage of the prestressing steel during Run 15.

Measured Strains for the Prestressing Steel

The strain-displacement relationships for strands 1, 2, 4 and 9 are shown in **Fig. 7**. The analytical results, which will be described in the section of Analytical Investigation, are also plotted. The abrupt strain reduction in strand No. 1 during Run 14 can be observed at the displacement of -61 mm (-2.4 in) due to the slippage. During Run 15, abrupt strain reductions can also be confirmed in strands 2 and 9. The average of the strains when the slippage occurred was $10550 \mu\epsilon$. From these results, it was possible to assume that the slippage would occur around the strain of $10500 \mu\epsilon$. The analytical results showed good correlation with the test results before the slippage occurred. Strand No. 4, which was at the centroid of the section, had no significant strain reduction after testing. In other words, strands No. 4 was still working well even after the test was completed; thus, it can be said that the prestressing steel at the web contributed to reducing the residual displacement at the end of the test.

Analytical Investigation

An analytical study was conducted to extend the scope of this research. A nonlinear push-over analytical model, using the finite element program called DIANA (TNO 2000), was calibrated with the load-displacement relationship from the test result.

A parametric study was carried out using push-over analysis. In the parametric study, the amount of the initial prestress, height of the column, depth of the section and the axial force due to the superstructure weight were taken as parameters. An equation to estimate the strain in the prestressing steel was proposed from the results of the parametric study. Finally, a simplified method to find the moment-drift relationship was determined.

Calibration Result

The push-over analysis was conducted by the displacement control method. The load-displacement relationship with the envelope of test result is shown in **Fig. 8**. The analytical model showed good correlation with the test result. Comparing the analytical result with the test result in the primary/negative direction, a slight difference at a displacement of 25 mm (1 in) can be observed. This was because the cover concrete in the analytical model completely spalled in the out-of-plane direction at the same time since the analytical model was two dimensional, while it gradually spalled in the test. At the displacement of 51 mm (2 in) where the prestressing steel yielded in the analysis, the force from the calibrated model matched with that of the test result well.

The failure point must be defined for a parametric study. It was conservative to define the failure as the point where the strain in the prestressing steel reached 10500 $\mu\epsilon$, since the specimen showed more ductility. This definition of the failure point will be applied for the parametric study. However, the failure does not indicate the ultimate displacement in real structures.

Parametric Study

A parametric study was conducted with a nonlinear push-over analysis. The scaling factor of the analytical model was one-fourth, which was identical to the specimen. The initial stress in the prestressing steel, height of the column, depth of the section and the axial force due to the superstructure weight were taken as the parameters. **Table 2** shows the analysis cases. The initial stress in the prestressing steel was selected at 20%, 40% and 60% of the ultimate strength, 1860 MPa (270 ksi). The heights of the columns were 1.83 m (6 ft), 3.66 m (12 ft), 5.49 m (18 ft) and 9.14 m (30 ft), which corresponded to 4, 8, 12 and 20 for the aspect ratio, respectively. The depths of the sections were 1.83 m (6 ft) and 3.66 m (12 ft), where the thickness of the flange was not changed but the height of the web was increased. The axial force due to the superstructure weight was set at 445 kN (100 kips), 890 kN (200 kips) and 1334 kN (300 kips), which corresponded to 5%, 10% and 15% of $f'c$ Ag.

Equation to Estimate Strain Change in the Prestressing Steel

Fig. 9 shows the strain-drift relationships of Cases 1 to 3 for the prestressing steel in the tension flange. The strain-drift relationship could be regarded as linear. The slopes were identical for all three cases. Most of the column displacement occurred due to the rotation of joint opening at the base of column; therefore, the elongation of the prestressing steel was linear to the drift.

Assuming that the slope of the strain-drift relationship is perfectly linear, Eq. (1) was developed by referring to the equation to estimate the stress in the prestressing steel at the ultimate condition (AASHTO 2002), where C is a coefficient to express the linear relationship.

$$\varepsilon_{ps} = \varepsilon_{pe} + C \left(\frac{d_i - t_f}{l_p} \right) x \leq 10500 \mu\varepsilon \quad (1)$$

where,

- ε_{ps} = strain in the prestressing steel, micro strain
- ε_{pe} = effective strain in the prestressing steel, micro strain
- d_i = depth of each prestressing steel
- t_f = thickness of the flange in compression
- l_p = length of the prestressing steel
- C = coefficient to represent the linear relationship = 1050000
- x = drift ratio = displacement / column height

To check the validity of Eq. (1), the results from the push-over analyses were compared with the results from Eq. (1) in **Fig. 10**. Eq. (1) showed good correlation with the analytical result, which could be applied for all other cases. For the cases investigated, it can be said that Eq. (1) has sufficient accuracy in terms of estimating the strain in the prestressing steel. The stress in the prestressing steel was calculated by using the prestressing strand stress-strain relationship provided by Caltrans (Caltrans 2004).

Conclusions

1. The specimen performed very well with essentially no residual displacement and only limited spalling at the base. The damage to the concrete could be easily repaired. A methodology for accessing the tendons would need to be developed for an actual bridge.
2. The slippage of the prestressing steel occurred around the strain of 10500 $\mu\varepsilon$. Due to the impact of the slippage, the anchorage plates popped out. The tendons would need to be replaced to complete column repair.
3. The prestressing steel at the centroid of the section worked well even after testing and contributed to reducing the residual displacement at the end of the test.
4. The joints between the first and the second segments and between the second and the third segments remained closed. All significant behavior occurred at the base of the first segment.
5. The calibrated model for the push-over analysis had good correlation with the test result.

6. An equation to estimate the strain in the prestressing steel in terms of the drift was proposed. The equation showed good correlation with the analytical result.

7. Design methodology and design limits are being developed.

Acknowledgments

Dywidag-Systems International, USA (DSI) is gratefully acknowledged for donation of the prestressing strands. General Technologies Inc (GTI) is acknowledged for their donation of the anchorage systems of the prestressing strands and technical support. Sika Corporation, USA is acknowledged for donation of the epoxy adhesive used in bonding the precast segments and technical assistance.

References

AASHTO, "Guide Specification for Design and Construction of Segmental Concrete Bridges", 2nd Edition, 1999.

AASHTO, "Standard Specification for Highway Bridges", 17th Edition, 2002.

AASHTO-PCI-ASBI, "Segmental Box Girder Standard for Span-by-Span and Balanced Cantilever Construction", Edition II, November 2002.

Caltrans, "Seismic Design Criteria Version 1.3", February 2004.

Laplace, P., Sanders, D., Saiidi, M., Douglas, B. and El-Azazy, S., "Performance of Concrete Bridge Columns under Shake Table Excitation", ACI Structural Journal, Vol. 102, No.3, May/June 2005, pp. 438-444.

TNO Building and Construction Research, "DIANA Release 7.2 User's Manual", 2000.

Yamashita, R. and Sanders, D., "Shake Table Testing and an Analytical Study of Unbonded Prestressed Hollow Concrete Columns Constructed with Precast Segments", Report No. CCEER 05-9, University of Nevada, Reno, 2005.

Table 1 Observed Behavior During Testing at Selected Runs

Run	PTA*	Max. Disp.	Force at Max. Disp.	Residual Disp.	Observed Behavior
5	0.83 g	18.5 mm (0.73 in)	266 kN (59.8 kips)	1.3 mm (0.05 in)	-Joint opening at the bottom of the column
11	0.64 g	23.9 mm (0.94 in)	283 kN (63.7 kips)	1.5 mm (0.06 in)	-First cover concrete crushing (south side)
12	0.65 g	26.2 mm (1.03 in)	289 kN (64.9 kips)	1.8 mm (0.07 in)	-Cover concrete crushing (north side)
13	1.01 g	38.4 mm (1.51 in)	303 kN (68.1 kips)	1.8 mm (0.07 in)	-First cover concrete spalling (north and south sides)
14	1.27 g	71.1 mm (2.80 in)	289 kN (64.9 kips)	2.8 mm (0.11 in)	-Cover concrete completely spalled (south side) -Anchorage of strand No.1 popped out
15	1.14 g	177 mm (6.96 in)	219 kN (49.3 kips)	3.0 mm (0.12 in)	-Cover concrete completely spalled (north side) -Damage of core concrete at corners -Anchorages of strand No.9 and No.11 popped out

* Peak table acceleration

Table 2 Analysis Cases

Case	Case name	Column height	Aspect ratio	Initial prestress	Section depth	Axial force
1	4-60-1	1.83 m (6 ft)	4	0.6 f_{pu}	0.46 m (1.5 ft)	445 kN (100 kips)
2	4-40-1			0.4 f_{pu}		
3	4-20-1			0.2 f_{pu}		
4	8-60	3.66 m (12 ft)	8	0.6 f_{pu}		
5	8-40			0.4 f_{pu}		
6	8-20			0.2 f_{pu}		
7	12-60	5.49 m (18 ft)	12	0.6 f_{pu}		
8	12-40			0.4 f_{pu}		
9	12-20			0.2 f_{pu}		
10	20-60	9.14 m (30 ft)	20	0.6 f_{pu}		
11	20-40			0.4 f_{pu}		
12	20-20			0.2 f_{pu}		
13	4-60-2	3.66 m (12 ft)	4	0.6 f_{pu}	0.91 m (3 ft)	
14	4-40-2			0.4 f_{pu}		
15	4-20-2			0.2 f_{pu}		
16	4-60-3	1.83 m (6 ft)	4	0.6 f_{pu}	0.46 m (1.5 ft)	890 kN (200 kips)
17	4-60-4					1334 kN (300 kips)

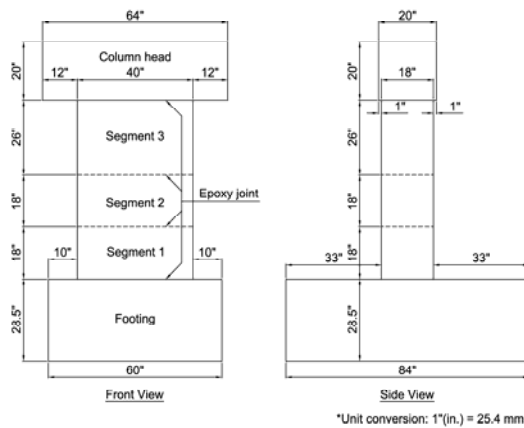


Fig. 1 Specimen Views

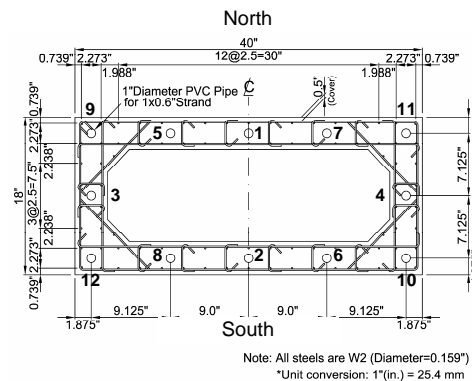


Fig. 2 Specimen Cross Section



Fig. 3 Test Setup

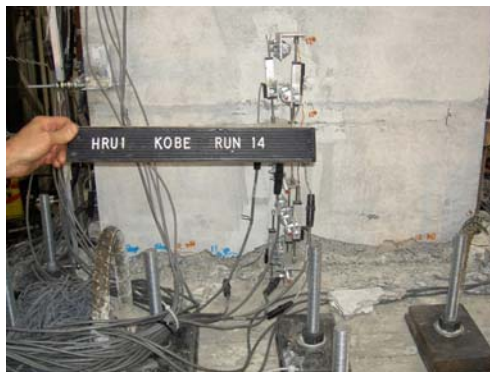


Fig. 4 Spalling Cover Concrete



Fig. 5 Anchorages After Test

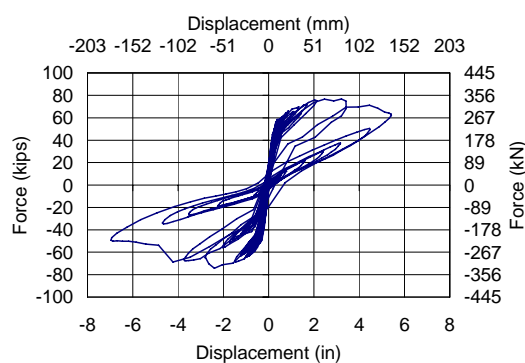


Fig. 6 Hysteresis Curve

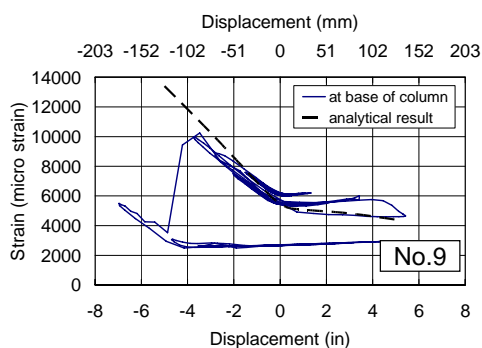
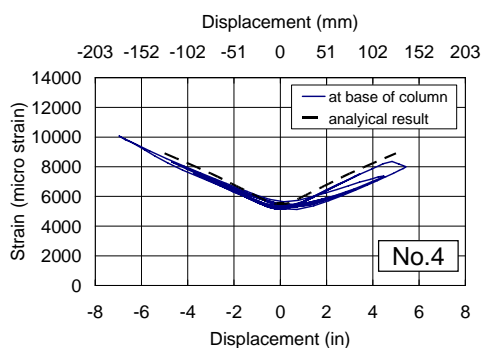
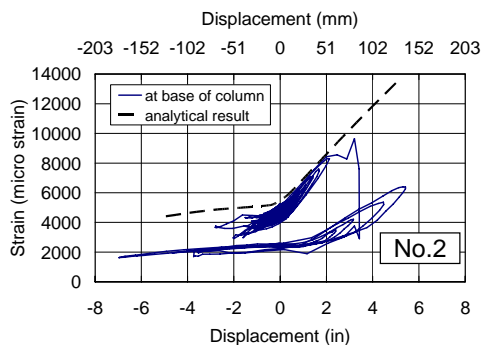
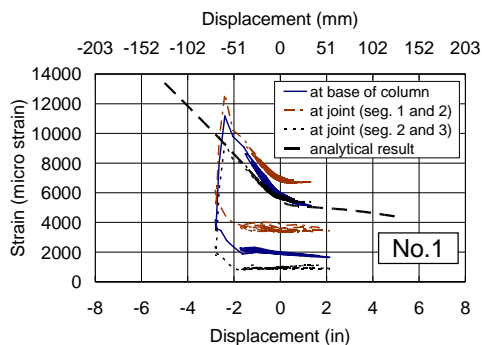


Fig. 7 Strain-Displacement Relationships

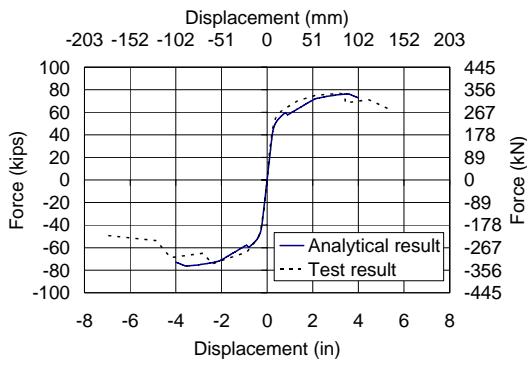


Fig. 8 Calibration Results

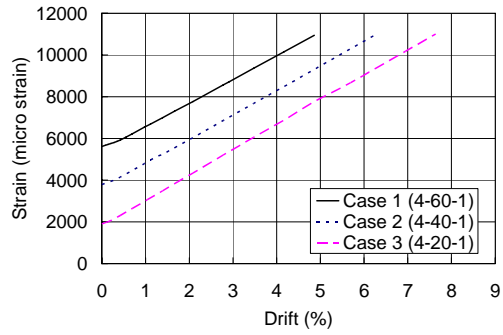


Fig. 9 Strain-Drift Relationships

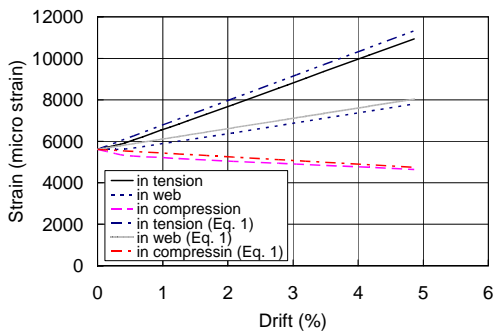


Fig. 10 Validation of Eq. (1)